



Carbon stock estimation by dual-polarized synthetic aperture radar (SAR) and forest inventory data in a Mediterranean forest landscape

Can Vatandaşlar¹ · Saygin Abdikan²

Received: 1 February 2021 / Accepted: 8 May 2021
© The Author(s) 2021

Abstract Forest ecosystems play a crucial role in mitigating global climate change by forming massive carbon sinks. Their carbon stocks and stock changes need to be quantified for carbon budget balancing and international reporting schemes. However, direct sampling and biomass weighing may not always be possible for quantification studies conducted in large forests. In these cases, indirect methods that use forest inventory information combined with remote sensing data can be beneficial. Synthetic aperture radar (SAR) images offer numerous opportunities to researchers as freely distributed remote sensing data. This study aims to estimate the amount of total carbon stock (TCS) in forested lands of the Kizildag Forest Enterprise. To this end, the actual storage capacities of five carbon pools, i.e. above- and below-ground, deadwood, litter, and soil, were calculated using the indirect method based on ground measurements of 264 forest inventory plots. They were then associated with the back-scattered values from Sentinel-1 and ALOS-2 PALSAR-2 data in a Geographical Information System (GIS). Finally, TCS was separately modelled and mapped. The best regression model was developed using the HH polarization of ALOS-2 PALSAR-2 with an adjusted R^2 of 0.78 ($p < 0.05$). According to the model, the estimated TCS was about

2 Mt for the entire forest, with an average carbon storage of 133 t ha^{-1} . The map showed that the distribution of TCS was heterogenic across the study area. Carbon hotspots were mostly composed of pure stands of Anatolian black pine and mixed, over-mature stands of Lebanese cedar and Taurus fir. It was concluded that the total carbon stocks of forest ecosystems could be estimated using appropriate SAR images at acceptable accuracy levels for forestry purposes. The use of additional ancillary data may provide more delicate and reliable estimations in the future. Given the implications of this study, the spatiotemporal dynamics of carbon can be effectively controlled by forest management when coupled with easily accessible space-borne radar data.

Keywords Carbon storage · Aboveground carbon · Soil-bound carbon · Forest biomass · Synthetic aperture radar (SAR)

Introduction

In response to human-induced global warming, many countries have participated in various international initiatives to reduce their greenhouse gas emissions (IPCC 2007; Sanquetta et al. 2011; UNFCCC 2016; FAO 2020). In the framework of these initiatives, the countries are requested to quantify and report periodically their greenhouse gas inventories as well as carbon stocks (Somogyi et al. 2007; FAO 2015; Njana 2017). Since atmospheric carbon dioxide (CO_2) is responsible for most greenhouse gas emissions, increasing the amount of CO_2 sequestered is seen as an effective strategy in reducing global warming. In this sense, having reliable information on CO_2 fluxes is essential to balance carbon budgets (Le Toan et al. 2011; Güner et al. 2021).

Project funding: No funding received for this study.

The online version is available at <http://www.springerlink.com>

Corresponding editor: Zhu Hong

✉ Can Vatandaşlar
canvatandas@hotmail.com

¹ Department of Forest Engineering, Artvin Coruh University, 08100 Artvin, Turkey

² Department of Geomatics Engineering, Hacettepe University, 06800 Ankara, Turkey

Through photosynthesis, forests absorb CO₂ in the atmosphere, convert it into carbon-based compounds, and store the carbon in woody biomass. Indeed, forests have the most significant carbon stock amongst terrestrial ecosystems; nearly 80% of carbon is stored in forest ecosystems worldwide (Jandl et al. 2007; Güner et al. 2021). Moreover, carbon can still be stored in wood products, even after harvesting (Saraçoğlu 2010). Therefore, forests play a key role in the global carbon cycle as both potential carbon sources and carbon sinks. On the one hand, fuelwood removals and deforestation are critical carbon sources due to their contributions to CO₂ emissions. And on the other hand, forests are considered significant carbon sinks since they can fix large amounts of carbon in their woody biomass (Hu and Wang 2008; Patel and Majumdar 2011; Mumcu Kucuker 2020). Thus, the smart management of carbon stocks in the forest is crucial for climate change mitigation. Accomplishing this task is closely related to quantifying the magnitude, spatial distribution, and change in forest biomass because roughly half of living biomass is composed of carbon (Le Toan et al. 2011; Njana 2017).

In forest ecosystems, carbon is stored not only in living (above- and below-ground) biomass but also in several carbon pools including soil, and dead organic matter (i.e., deadwood and litter) (IPCC 2006; Erkan et al. 2020). Each pool contributes a certain proportion to the total carbon stock (TCS) in the ecosystem. In the world's forests, carbon proportions stored in living biomass, soil organic matter, and dead organic matter are about 45%, 45% and 10%, respectively (FAO 2020). In some northern countries, the proportion of carbon stored in the soil can be much more than stored in other pools. In Finland, for example, the amount of carbon stored in the forest soil is about 4×10^6 t while it is only 0.78×10^6 t in living biomass (FAO 2015). Therefore, the contribution of each carbon pool needs to be taken into account in quantification studies. In this respect, Earth observation through remote sensing offers researchers invaluable opportunities for geospatial data acquisition, mapping, monitoring, and dissemination of results. Given a world facing risks by climate change, this is also true for achieving the Sustainable Development Goals described under the United Nations for the 2030 Agenda (UN 2015; Anderson et al. 2017; FAO 2020).

The Japanese Aerospace Exploration Agency (JAXA) is one of the supporters of the Earth observation strategies. For this purpose, the ALOS Kyoto & Carbon Initiative has been developed to support data and information derived from L-band synthetic aperture radar (SAR) sensors. In fact, SAR systems provide higher sensitivity to geometric attributes of forest structure than optical systems (Gao et al. 2018; Sun and Liu 2020). Moreover, they can acquire imagery both day and night regardless of unfavourable weather conditions such as cloud cover

or lack of illumination. SAR systems acquire images at a side-looking direction that transmits microwave energy and receives the backscattered signal from the Earth's surface. The benefit of a SAR system for large area mapping depends on several parameters. One of the important ones is the wavelength of the system. The frequency of the signal determines the wavelength of the electromagnetic wave that interacts with objects. In particular, L-band ALOS is widely preferred due to its longer wavelength, which can better penetrate vegetation cover and interact with large branches and trunks than shorter wavelengths (Thapa et al. 2015). A strong volumetric scattering from the vegetation is expected when the wavelength of a SAR sensor has a similar size to the plant components (Lillesand et al. 2015). Thus, many studies have been conducted using ALOS data for estimating aboveground carbon stock in tropical forests (Morel et al. 2011; Hamdan et al. 2014; Thapa et al. 2015; Behera et al. 2016; Sinha et al. 2019).

Copernicus is another Earth observation initiative launched by the European Space Agency (ESA). Its Sentinel-1 mission has distributed SAR data online and free of charge since 2014. Unlike ALOS, Sentinel-1 uses C-band SAR imaging (ESA 2020). C-band (~6 cm) can also penetrate through crowns and detect backscatter of medium branches and trunks, whereas X-band (~3 cm) SAR signals mostly backscatter from the top of the canopies, thin branches and leaves. Another important parameter of the system is polarimetry. It describes the direction of the plane that a transmitting and/or received signal oscillates. Most of the sensors have linear polarimetry, and they transmit signals horizontally (H) and/or vertically (V). The images with cross-polarized data that are vertically transmitted and horizontally received (VH) or horizontally transmitted and vertically received (HV) represent stronger volumetric backscatter than co-polarized (VV and HH) data (Meyer 2019). Even cross-polarized SAR images provide better information on biomass than other polarization in general, Sinha et al. (2018) showed that HH polarization resulted in a higher relationship with aboveground biomass than cross-polarized data of C-band Radarsat-2. The C-band SAR is mostly used for estimating aboveground forest biomass in the tropics (Omar et al. 2017; Liu et al. 2019; Navarro et al. 2019; Nuthammachot et al. 2020). In general, it is understood that most of the forest-related SAR studies have been conducted in tropical and subtropical domains with a focus on aboveground carbon pools. It is attributable to ongoing deforestation, whose rate is the highest in tropical forests in the world (FAO 2020). In fact, tropical deforestation is responsible for about 98% of land-use-change CO₂ flux, converting biomass carbon into emissions (IPCC 2007; Le Toan et al. 2011). Nevertheless, climate change also deeply affects forests in arid and semi-arid regions (Allen et al. 2010). However, to our knowledge, there is no SAR study focused on TCS in

dry forest ecosystems, which are possibly more vulnerable to climate change.

Therefore, the major objective of this study is to estimate TCS (i.e., the sum of living biomass, deadwood, litter, and soil-bound carbon) in an arid Mediterranean forest environment using SAR sensors. The secondary objectives are: (1) to compare the estimation accuracies achieved by different sensors (ALOS-2 PALSAR-2 and Sentinel-1), bands (L- and C-bands), and polarizations (HH, HV, VV and VH); and, (2) to determine the carbon hotspots across the study area. To this end, regression models were developed for each sensor based on the inventory data measured from 264 forest sample plots. Accordingly, two maps were produced by ALOS-2 and Sentinel-1 imageries for demonstrating the distribution of TCS in the Kizildag Forest Enterprise. The present study provides spatially explicit information on the magnitude and distribution of carbon stored in a semi-arid forest landscape in southern Turkey. Forest management planners, remote sensing professionals, and climate scientists are expected to benefit from the results of the present study.

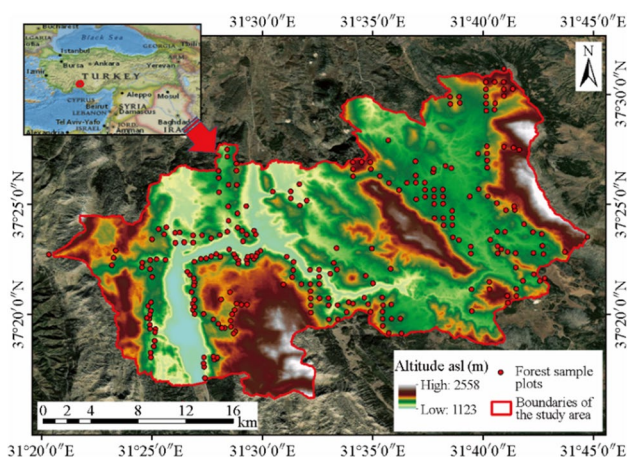


Fig. 1 General view of the study area

Table 1 Area cover of LULC classes in the Kizildag Forest Enterprise (GDF 2016)

Land use land cover (LULC) class	Area (ha)	Proportion tototal area (%)
Forest *	20,140	37.8
Other wooded land (OWL) (i.e., degraded forests, forest openings, bare forest soil) *	19,152	35.9
Agricultural land	8758	16.4
Steppe	1687	3.2
Other classes (settlements, rocky areas, water bodies, etc.)	3553	6.7
Total	53,290	100.0

(*) FAO's definitions were used in separating the forest and other wooded lands (OWL) in the study area (i.e., the forest refers to 'land with a tree canopy cover of more than 10% and area of more than 0.5 ha')

Materials and methods

Study area

The study area is Kizildag Forest Enterprise, located in the Western Mediterranean sub-region of Turkey (Fig. 1). It has a mountainous landscape (average slope > 30%) with an area of 53,290 ha. The climate in the region is transitional between continental and Mediterranean. Accordingly, the annual averages of temperature and total precipitation are 11.5 °C and 329 mm, respectively. Rain falls in the winter season during December and January. Drought has a profound impact on most parts of Kizildag, particularly in the growing season. Thus, the region is classified as arid based on Erinç's aridity index (Erinç 1984; Dinç and Vatandaşlar 2019). According to Ozkan et al. (2007), brown forest soils are ubiquitous in the forested lands of the basin where Kizildag is located.

Table 1 shows land use and land cover (LULC) classes of the study area by their area. In Kizildag, all forests are (semi-)natural, accumulating in mountainous lands with almost no human-induced disturbances. The flatter lowlands are dominated by agricultural areas and anthropogenic steppes (GDF 2016). Pure and mixed conifer stands are dominant in the study area. The main tree species are Anatolian black pine (*Pinus nigra* Arnold subsp. *pallasiana* (Lamb.) Holmboe), Lebanese cedar (*Cedrus libani* A. Rich.), Taurus fir (*Abies cilicica* (Antoine & Kotschy) Carrière), and juniper (*Juniperus* spp.) in descending order by their area. Nevertheless, forest stands seldom fully cover the soil surface, and forest fragmentation is a critical issue in most parts of the landscape.

Remote sensing instruments and data processing

C-band Sentinel-1 and L-band ALOS-2 PALSAR-2 data were used. ALOS-2 is a dual polarimetric mosaic that had HH and HV data provided by the JAXA. The L-band (22.9 cm wavelength) ALOS-2 data consisted of 10 × 10

degree mosaic tiles for the year 2015 (Shimada et al. 2014). The pre-processing steps (radiometric and geometric corrections) have been applied by JAXA, and the data is freely distributed with 25 m-resolution pixel size.

The C-band (5.5 cm wavelength) Sentinel-1 image was acquired on June 19th 2015 in Interferometric Wide Swath mode and descending orbit. The Ground Range Detected High Resolution (GRDH) level data has VV and VH polarization. The Sentinel Application Platform (SNAP) software was utilized for the pre-processing steps shown in Fig. 2 (SNAP 2019). Specifically, precise orbit files were first used to update the satellite position accurately. Then, thermal noise removal was applied to reduce its effect. Radiometric calibrated values were extracted using digital number (DN) values of each pixel. To increase the image quality, the gamma map filter that was successful over forested regions in previous studies was applied to reduce the speckle effect in 5×5 kernel sizes (Abdikan 2018; Nuthammachot et al. 2020). The study area has a hilly topography. As the SAR systems acquire the image at the line of sight direction, it will be affected by slope and the look angle. To reduce distortions due to terrain variation on backscatter, a radiometric terrain flattening step was applied (Meyer 2019; Nuthammachot et al. 2020). Finally, Range Doppler terrain correction was implemented using Shuttle Radar Topography Mission (SRTM) 1 Sec data. The Sentinel-1 data has a default pixel size at 10 m resolution.

Calculation of stocks in different carbon pools

The direct and indirect methods are two approaches in calculating biomass and carbon stocks in a forest ecosystem. The direct method is based on destructive sampling, biomass weighing, and developing allometric biomass equations from the destructively sampled data. The indirect method, on the other hand, is much more practical and is generally used when there are no biomass equations at hand (Hu and Wang 2008; Njana 2017). This method is based on forest inventory data and various coefficients such as biomass expansion factors, root-to-shoot ratios, and carbon fractions of dry matter (IPCC 2006; Somogyi et al. 2007; Mumcu Kucuker 2020).

Since there was no reliable biomass equation for dominant tree species in our study area, we used the indirect method for calculating TCS in the forest ecosystem (Fig. 2). To this end, a volume-based forest inventory data (GDF 2016) was utilized. Accordingly, a comprehensive timber survey was carried out in the Kizildag Forest Enterprise under the supervision of the General Directorate of Forest (GDF) in 2015. A total of 264 sample plots were systematically distributed to forested areas with an equal interval of about $300 \text{ m} \times 300 \text{ m}$ (Fig. 1). The plots were circular with sampling sizes of 400, 600, or 800 m^2 , depending on the canopy closure. All plots were identified by forestry professionals using a handheld GPS. The diameter at breast height (dbh) and dominant tree heights were measured for trees $\geq 8 \text{ cm}$ dbh. Tree species, canopy closure, and tree health were also observed and recorded into inventory

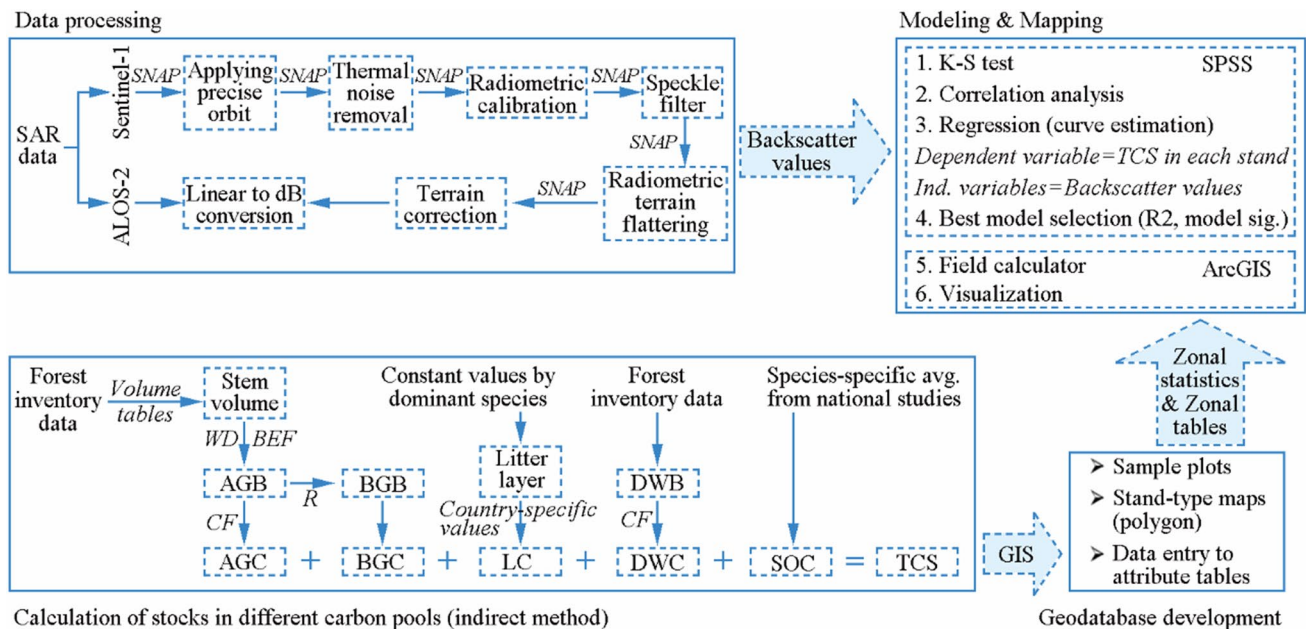


Fig. 2 Flowchart of the study (WD is species-specific wood density values; BEF: biomass expansion factor; AGB: aboveground biomass; CF: carbon fraction of dry matter; AGC: aboveground carbon; R:

root-to-shoot ratios; BGB: belowground biomass; BGC: belowground carbon; LC: litter carbon; DWB: deadwood biomass; DWC: deadwood carbon; SOC: soil organic carbon; TCS: total carbon stock)

sheets. Further information on the timber survey can be found in the national guideline (GDF 2017).

In a next step, aboveground biomass (AGB) was determined and for this purpose, the merchantable stem volume of each tree was first calculated based on species-specific local volume tables (GDF 2016). Species-specific wood density values were then used to calculate stem biomass which excludes biomass from other tree components such as foliage, branches, fruits, and cones. Therefore, the wood density are multiplied by a biomass expansion factor to obtain the AGB value. Species-specific biomass expansion factors developed by Turkish researchers based on nearby field studies were used (Tolunay 2009, 2011). After this step, single-tree AGBs were aggregated to the plot, stand, and unit area (i.e., 1 ha), as described in the GDF (2017).

Once the amount of AGB is known, it is possible to derive the value of belowground biomass (BGB) based on root-to-shoot (R) ratios (IPCC 2006; Tolunay 2011). These ratios differ by ecological zones, forest cover types, and the amount of AGB (Table 2). Regarding the litter layer, constant values for dry weight and organic matter were used according to dominant tree species. The area-specific values suggested for Turkey's main tree species are in Tolunay and Çömez (2008). Lastly, deadwood biomass was directly obtained from the forest inventory data for each plot (Fig. 2).

The last step consists of calculating the amount of carbon stored in the above-mentioned pools separately. To this end, Eqs. 1 and 2 were used for determining the carbon stocks in both conifer and broadleaved AGB (IPCC 2006). Likewise, belowground carbon stock was calculated with the same coefficients given in Eqs. 1 and 2. As for litter carbon, species- and country-specific values were directly used based on the dominant tree species in forest stands. These values were derived from the national studies reviewed by Tolunay and Çömez (2008) in detail. Equation 3 was used for calculating carbon stock in deadwood regardless of tree species (FAO 2010; GDF 2017). On the other hand, the species-specific averages suggested in the literature were used for

determining the amount of organic carbon stored in forest soil (Tolunay and Çömez 2008). Finally, TCS in the whole forest ecosystem was calculated by summing up all the various carbon pools, as formulated in Eq. 4:

$$A_{GCC} = A_{GB} \times C_{FC} \quad (1)$$

$$A_{GCD} = A_{GB} \times C_{FD} \quad (2)$$

$$D_{WC} = D_{WB} \times C_{FDW} \quad (3)$$

$$T_{CS} = A_{GC} + B_{GC} + L_C + D_{WC} + S_{OC} \quad (4)$$

where, A_{GCC} and A_{GCD} are the carbon stocks in conifer and deciduous forest biomass; C_{FC} , C_{FD} , C_{FDW} are the carbon fraction in A_{GBC} , A_{GBD} , and deadwood (Table 2). D_{WC} and D_{WB} are the deadwood carbon and deadwood biomass. T_{CS} , B_{GC} , L_C , and S_{OC} are the total carbon stock, belowground carbon, litter carbon, and soil organic carbon, respectively.

Spatial analyses and modelling

A geodatabase was first developed in the GIS environment, compiling a stand-type map, sample plots, DEM, and study area boundaries. Necessary inventory variables such as stand volume, species mix, and deadwood were entered in the stand type map's attribute table. Similarly, stocks calculated in different carbon pools (i.e., AGB, BGB, litter, deadwood, and soil) were separately entered at the stand (sub-compartment) level (Fig. 2).

After geodatabase development, radar imageries were laid out along with the stand type map. The 'zonal statistics' function was used for extracting the sum of backscattered values of the Sentinel-1 and ALOS-2 PALSAR-2 images within each sub-compartment. 'Zonal tables' were then joined to the attribute table of the stand type map based on the 'field ID' column in ArcGIS.

Table 2 Root-to-shoot (R) ratios and carbon factors used in this study (Lamloom and Savidge 2003; IPCC 2006; Mokany et al. 2006; FAO 2010)

Ecological zone	Forest cover type	The amount of AGB (t ha ⁻¹)	BGB to AGB ratio (R)	Carbon fraction of dry matter
Temperate forests including oceanic, continental, and mountain systems	Deciduous (broadleaved canopy)	< 75	0.46	0.48 (0.46–0.50)
		75–150	0.23	
		> 150	0.24	
	Coniferous (evergreen canopy)	< 50	0.40	0.51 (0.47–0.55)
		50–150	0.29	
		> 150	0.20	
Deadwood (deciduous or conifer)	N/A	N/A	0.47	

AGB is aboveground biomass; BGB is belowground biomass; R is root-to-shoot ratio

Next, all values in the attribute table were transferred into an Excel sheet. They were first subjected to the Kolmogorov–Smirnov test and Pearson’s correlation analysis in SPSS software ($p < 0.05$). The variables strongly correlated with backscattered values were determined both for the forest class and forest, and OWL classes together. Subsequently, the simple linear regression method was used to plot and estimate the curve relationships between carbon stocks in each sub-compartment and backscattered values from satellite data. The best model curves for each satellite image were chosen based on the coefficient of determination (R^2), the significance of the model and its coefficients (β_1, β_2 , etc.), and ease of mapping (e.g., if their R^2 values were equal, ‘the linear model’ was preferred against ‘the cubic’ since it had fewer coefficients).

In ArcGIS, the best models were entered into the ‘field calculator’. Here, TCS in each sub-compartment was the dependent variable, while backscatter values from VH and HH polarizations of Sentinel-1 and ALOS-2 were the independent variables. Thus, TCS of the forested land was modelled and mapped for the Kizildag Forest Enterprise. All methodology of the study is in Fig. 2 with a workflow diagram.

Results

Correlations among various carbon pools and SAR data

Correlation coefficients for each carbon pool and SAR data are documented in Table 3. As for Sentinel-1 data, the VH

polarization showed stronger correlations than the VV for almost all pools. The highest coefficient was observed between soil organic carbon (SOC) content and the VH polarization in the forest class ($r = -0.97, p < 0.01$). The lowest, but still significant, coefficient was between deadwood carbon (DWC) and the VH polarization for the forest + OWL classes together ($r = -0.19, p < 0.01$). In general, correlation coefficients further increased when the forest class was evaluated separately (Table 3). All carbon pools together showed a negative and strong correlation between TCS and the VH polarization with an r -value of more than 0.80 ($p < 0.01$).

As for ALOS-2 data, the correlation coefficients were similar to those of Sentinel-1. The HH polarization better correlated with several carbon pools than the HV polarization. The highest coefficient was 0.93 between SOC and the HH polarization for the forest class ($p < 0.01$). Regarding TCS, it was 0.88 for the same polarization in the same LULC class ($p < 0.01$). As with Sentinel-1 data, correlations in ALOS-2 data were stronger for the forest class than those for the forest + OWL classes together. Thus, TCS was modelled only for the forest class using Sentinel-1’s VH and ALOS-2’s HH polarizations.

Regression models for estimating total carbon stock

Since there are numerous carbon pools, SAR data, and LULC classes, only TCS was modelled for the forest LULC class based on the strong correlations between the relevant variables. Table 4 demonstrates nine regression models using Sentinel-1’s VH polarization as an independent variable. Accordingly, all models except for cubic were statistically

Table 3 Correlations (r -values) between various carbon pools and SAR data

SAR data	LULC class	Polarization	AGC	BGC	DWC	LC	SOC	TCS
Sentinel-1	Forest	Vertically transmitted and vertically received	-0.60**	-0.42**	-0.35**	-0.76**	-0.93**	-0.84**
		Vertically transmitted and horizontally received	-0.58**	-0.43**	-0.39**	-0.80**	-0.97**	-0.86**
	Forest + OWL***	Vertically transmitted and vertically received	-0.37**	-0.24**	-0.19**	-0.80**	-0.92**	-0.83**
		Vertically transmitted and horizontally received	-0.35**	-0.24**	-0.20**	-0.83**	-0.95**	-0.85**
ALOS-2	Forest	Horizontally transmitted and horizontally received	0.67**	0.53**	0.48**	0.89**	0.93**	0.88**
		Horizontally transmitted and vertically received	0.28**	0.28**	0.55**	0.31**	0.05*	0.31**
	Forest + OWL***	Horizontally transmitted and horizontally received	0.47**	0.36**	0.32**	0.88**	0.90**	0.86**
		Horizontally transmitted and vertically received	0.39**	0.39**	0.58**	0.42**	0.28**	0.42**

AGC, above ground carbon; BGC, below ground carbon; DWC, deadwood carbon; LC, litter carbon; SOC, soil organic carbon; TCS, total carbon stock; OWL, other wooded land; (*) the correlation between the variables is statistically meaningful at the 0.05 significance level; (**) the correlation between the variables is statistically meaningful at the 0.01 significance level; (***) the definitions for forest and OWL classes are given in Table 1. (****) The highest r values were formatted as bold for TCS

Table 4 Regression models using Sentinel-1's VH polarization for estimating total carbon stocks in the forest

Model type	Model coefficients				R^2_{adj}	p -Value
	β_0	β_1	β_2	β_3		
Linear	145.5	-0.051			0.74	<0.05
Inverse	1434.8	2,827,167.0			0.24	<0.05
Quadratic	46.3	-0.063	-0.00000015		0.74	<0.05
Cubic	-26.2*	-0.076	-0.000001	-0.00000003	0.75	<0.05
Compound	296.8	0.999			0.54	<0.05
S curve	7.1	4410.1			0.65	<0.05
Growth	5.7	-0.000042			0.54	<0.05
Exponential	296.8	-0.000042			0.54	<0.05
Logistic	0.003	1.0			0.54	<0.05

(*) The standard error of the coefficient is statistically significant ($p < 0.05$); (**) the selected model is formatted as bold

meaningful. However, the standard error of β_0 of the cubic model was statistically significant ($p < 0.05$). Excluding this model, the highest adjusted coefficient of determination (R^2) was in both linear and quadratic models ($R^2 = 0.74$). Since the linear model had a simpler equation, it was selected to estimate and map TCS in the study area. The model can be formulated as Eq. 5:

$$T_{CS} = 145.535 - 0.051 \times V_H \quad (5)$$

where, T_{CS} is total carbon stock in the forest, and V_H is the backscattered value in the V_H polarization of Sentinel-1 data.

Regarding ALOS-2, developed models are shown in Table 5. The cubic model was excluded because the standard error of its β_2 coefficient was statistically significant ($p < 0.05$). Thus, linear and quadratic models showed the best performance with the same R^2 value of 0.78. As for the Sentinel models, the linear equation was chosen for modelling TCS. The model equation is given in Eq. 6 as follows:

$$T_{CS} = 172.768 + 0.241 \times H_H \quad (6)$$

where, T_{CS} is total carbon stock in the forest and H_H is the backscattered value in the H_H polarization of ALOS-2 data.

Quantity and spatial distribution of total carbon stock

Figure 3 depicts the quantity and spatial distribution of TCS in forest stands. This map was generated using Sentinel-1 data at the sub-compartment level. Accordingly, carbon stock per unit area ranged from 76.4 t ha⁻¹ in sparsely-covered areas on rocky sites to 381 t ha⁻¹ in fully-covered areas located on good sites. While the average carbon stock was 129.7 t ha⁻¹, the total amount of carbon stored in the entire forest was approximately 2.04 × 10⁶ t (Table 6). The spatial distribution of TCS was quite heterogenic across the landscape. In general, the eastern portion of the study area had more stored carbon than the western parts. Carbon hot-spots are shown in green (Fig. 3). The hotspots were mostly composed of pure stands of Anatolian black pine and mixed stands of cedar-fir in their mature age classes.

In terms of carbon stocks, the map derived from ALOS-2 data showed a more heterogenic pattern than Sentinel-1's

Table 5 Regression models using ALOS-2's HH polarization for estimating total carbon stock in the forest

Model type	Model coefficients				R^2_{adj}	p -Value
	β_0	β_1	β_2	β_3		
Linear	172.8	0.241			0.78	<0.05
Inverse	970.8	-23.5			0.01	<0.05
Quadratic	141.4	0.26	-0.000001		0.78	<0.05
Cubic	134.1	0.27	-0.000002*	0.0000001	0.78	<0.05
Compound	308.4	1.0			0.54	<0.05
S	6.4	-33.7			0.03	<0.05
Growth	5.7	0.0002			0.54	<0.05
Exponential	308.4	0.0002			0.54	<0.05
Logistic	0.003	1.0			0.54	<0.05

(*) the standard error of the coefficient is statistically significant ($p < 0.05$); (**) the selected model is formatted as bold

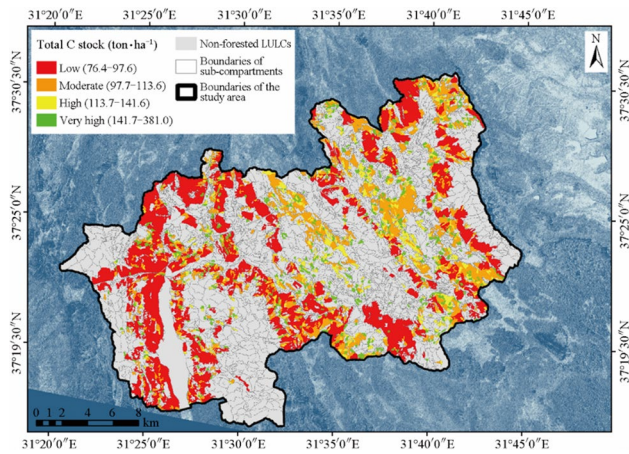


Fig. 3 Spatial distribution of total carbon stock in forested lands via Sentinel-1 data

Table 6 Estimated carbon stocks for forested lands of the Kizildag Forest Enterprise

SAR data	The amount of carbon stored per unit area ($t\ ha^{-1}$)			Total carbon stocking (t)
	Minimum	Average	Maximum	
Sentinel-1	76.4	129.7	381.0	2,041,582.2
ALOS-2	0.9	133.0	447.0	2,034,593.6

SAR is Synthetic Aperture Radar; ALOS-2 is Advanced Land Observing Satellite

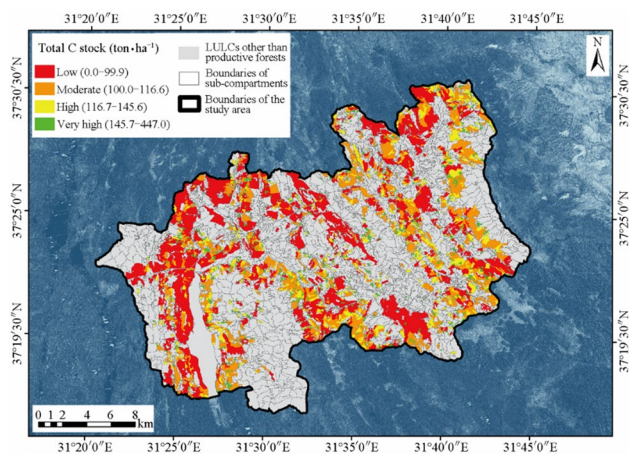


Fig. 4 Spatial distribution of total carbon stock in forested lands via ALOS-2 data

(Fig. 4). According to Table 6, total carbon stored in the entire forested lands was nearly 2.03 Mt. Carbon stock per unit area ranged from a few tons on newly regenerated and afforested sites to $447\ t\ ha^{-1}$ in mature, mixed stands of cedar-fir. The average of TCS was $133\ t\ ha^{-1}$ for the forest

class, close to that calculated from the Sentinel-1 data (Table 6). However, apparent differences were observed between the two maps regarding the spatial pattern. The left half of Fig. 4, in particular, is dissimilar from Fig. 3. The mixed and mature coniferous stands in these sections were estimated to store more carbon than as estimated by Sentinel-1 data. Carbon hotspots in Fig. 4 showed a scattered pattern along the landscape. In addition to the conifers, afforested sites of Turkey oak (*Quercus cerris* L.) also stored a large amount of carbon per unit area. However, their total area was limited in the Kizildag Forest Enterprise.

Discussion

In this study, the TCS of Kizildag's forests was estimated using SAR images from Sentinel-1 and ALOS-2 satellites. The performances of the two were almost the same with slight differences. Regardless which satellite data was selected, it was estimated that about 2 Mt of carbon was stored in the forestlands of the Kizildag Forest Enterprise. The average TCS was $129.7\ t\ ha^{-1}$. In Turkish forest management, carbon storage, carbon accumulation, and oxygen production capacities of each forest enterprise are periodically calculated and reported to international bodies for the global carbon budget (GDF 2017). In the Kizildag forest management plan, a total of 2.18 Mt carbon is estimated to be stored with an average of $110\ t\ ha^{-1}$ (GDF 2016). In another study conducted in the same enterprise, it was reported that the TCS was 1.97 Mt with an average of $120.8\ t\ ha^{-1}$ (Dinç and Vatandaşlar 2019). Thus, our estimation fell between the values reported in the literature. Slight differences can often be attributed to calculation procedures. Specifically, the amount of living biomass is calculated for each stand based on a rough classification as conifer and/or deciduous forests in Turkish forest management plans. In contrast, we used species-specific wood density and biomass expansion factors for calculating the biomass of several tree components (branches, leaves, and cones). In fact, wood density values for some tree species may vary considerably. Tolunay (2011), for example, reported wood density values for poplar (*Populus* spp.) and hornbeam (*Carpinus* spp.) as 0.35 and $0.63\ t\ m^{-3}$, respectively. Instead of using these values, taking a fixed amount for all deciduous trees would contribute to under- or over-estimating forest carbon stocks, as stated by Njana (2017) and Mumcu Kucuker (2020). Therefore, researchers should use species-specific values from local studies rather than the fixed averages suggested for conifer and deciduous forests (GDF 2017). Another difference in the present study is in the calculation of DWC. In earlier studies, the contribution of deadwood to TCS was either neglected (Sivrikaya et al. 2013; Günlü and Ercanlı 2018), or assumed as 1% of the total AGB in a given stand (Değermenci and

Zengin 2016; Mumcu Kucuker 2020). Instead, our calculation was based on the actual deadwood amount in each plot, thanks to up-to-date forest inventory data. This may be one of the earliest studies considering the actual amount of deadwood on the ground.

Using various remote sensing products, there are numerous studies modelling forest biomass and carbon stored in different pools of forest ecosystems (Le Toan et al. 2011; Günlü and Ercanlı 2018; Pham et al. 2018; Hernando et al. 2019; Mumcu Kucuker 2020). Günlü and Ercanlı (2018), for example, used ALOS PALSAR data to estimate carbon stocks in AGB of Oriental beech (*Fagus orientalis* L.) stands in northern Turkey. In order to develop a robust model, they tried several modelling techniques using different polarizations, texture features, and topographic parameters as independent variables. Their best model was developed using an artificial neural network technique with HH polarization. However, they concluded that the model performance remained mediocre ($R^2 = 0.53$). Our regression models, on the other hand, showed an acceptable performance ($R^2 = 0.74 - 0.78$) using only one independent variable. The difference between the model performances of the two studies can be attributed to a number of reasons. First, Günlü and Ercanlı (2018) modelled carbon stocks only in one pool, AGC. In the present study, however, five carbon pools were considered, and their sum (TCS) was modelled. Table 3 indicates that considering SOC and LC stocks positively affected our model accuracy. Their strong correlations with satellite data may be caused by bare lands in large forest openings in Kizildag. Secondly, the study areas were dissimilar in terms of site and forest settings. Günlü and Ercanlı (2018) study area, Göldağ, Sinop Province, located in the Black Sea region, is moist and a highly productive part of Turkey. Kizildag, Konya Province, on the other hand, is located in a relatively arid and poor area between the Mediterranean and Central Anatolia regions. Göldağ's forests are dominated by fully-stocked stands, possibly resulting in a signal saturation effect. In fact, the saturation effect is an important constraint of SAR data, particularly in dense forest environments (Cohen and Spies 1992; Hernando et al. 2019). Another reason could be different tree species studied. Günlü and Ercanlı (2018) studied only pure stands of Oriental beech. There was no information on the exact date of the acquisition of satellite data. But if taken in fall or winter, it might hinder the model performance due to the bareness of deciduous tree species. In contrast, the forestlands in this study were mostly evergreen species. Hence, our results could be positively affected by the distinct reflectance characteristics of conifers. However, both studies suggest that using the HH polarization of ALOS-2 data would be a good choice in estimating forest carbon stocking.

The amounts of carbon stored in various forest stands differed across the study area depending on biophysical

parameters (i.e., timber volume, tree species, canopy closure, developmental stage) and site condition. In the Kizildag Forest Enterprise, carbon stocks in mixed stands of mature, closed canopy conifers were more extensive than those of sparse pure stands located on poor sites. The eastern parts of the study area stored more carbon partly due to the differences in elevation. Mean elevation generally increases from west to east in Kizildag. Thus, the eastern highlands received more precipitation than the lowlands of the western areas. Tree growth was rarely limited by water deficits, resulting in fully-stocked forest stands in eastern Kizildag. In fact, it was clear that productive high forests were located on the right half of the stand type map (GDF 2016). Nevertheless, the carbon maps produced by this study present only a 'snapshot' of the forest landscape. The spatial pattern of forest carbon stocks may substantially change over time. Therefore, carbon dynamics of forested landscapes should be analysed periodically, as done by Değermenci and Zengin (2016) and Mumcu Kucuker (2020).

Our methodological approach in calculating carbon stocks was based on the amount of timber volume (growing stock). While forest carbon stocking is critical for climate change research (Saatchi et al. 2011; Baskent 2019), accurate information on timber volume and biomass is essential in both forest inventories and forest management (Hernando et al. 2019; Wan et al. 2019). Detailed field measurements are performed during timber surveys for deriving timber volume via tree dbh. Plot-based data are then extrapolated to larger scales for calculating the estate of forest enterprises, as well as the sustained yield of wood production (Vidal et al. 2016). Therefore, radar satellites can be used more effectively as a supporting tool for timber volume and forest biomass estimates. Thus forest management and inventory studies may also benefit from the present study's approach and models. However, one should keep in mind that these radar-based biomass estimates may show $\pm 20\%$ uncertainty as highlighted by Le Toan et al. (2011). Nevertheless, this rate is somewhat acceptable for many studies in practical forestry (Chave et al. 2004; Le Toan et al. 2011).

Conclusions and suggestions

Most studies use optical remote sensing for estimating forest biomass and carbon stocks. However, it may fail, especially in tropical regions where carbon stock is high and atmospheric conditions do not allow optical data use. In contrast, microwave SAR remote sensing provides cloud-free data for effective forest monitoring. This study estimated total carbon stocks of a typical Mediterranean forest ecosystem using freely distributed SAR images. It was found that approximately 130 t ha^{-1} carbon could be stored in aboveground, belowground, deadwood, litter, and soil

pools. The modelling results indicated that both L-band ALOS-2 and C-band Sentinel-1 data allowed satisfactory estimations based only on forest inventory information. Yet, HH polarization of the ALOS-2 data was a slightly more robust estimator ($R^2 = 0.78$) than VH polarization of the Sentinel-1 ($R^2 = 0.74$). The correlation between SAR data and soil organic carbon stock was stronger than in any carbon pools in the forest ecosystem. Studies to estimate forest carbon stock from SAR data are mostly considered to be AGC belonging to tropical forests. In the literature, limited studies address the potential of dual-polarized SAR for total carbon stock estimations for a semi-arid environment vulnerable to global warming. Considering the forest class alone generally yielded more accurate estimates compared to other LULC combinations, including the forest and OWL classes together.

The maps developed by this study showed that the distribution of total carbon stocks was heterogenic across the landscape. Carbon hotspots were distributed in the Kizildag Forest Enterprise in a patchwork pattern generally composed of pure stands of Anatolian black pine in managed forests and mixed, over-mature stands of cedar-fir in unmanaged forest compartments. This suggests that carbon dynamics and spatial patterns of carbon storage can be regulated by forest management. Setting appropriate management objectives, correct land-use allocations, and timely silvicultural interventions are useful practices applicable at the stand level. More specific recommendations may be made for field foresters, forest managers, and remote sensing professionals:

- (1) Biomass productivity could be increased by regenerating over-mature natural forests with the same tree species, even in areas allocated for environmental protection in the Kizildag Forest Enterprise;
- (2) Sparsely covered stands and OWL (e.g., degraded forests, forest openings) should be rehabilitated or reforested with native species with high yield capacity;
- (3) Industrial plantations should be established with fast-growing species (e.g., poplar, willow) on available bare lands along the rivers. The Kimyos plain is one of the suitable places in Kizildag;
- (4) Foresters may select flatter sites with no or little water deficit for afforestation. If this is impossible, drought-tolerant species should be used (e.g., juniper, oak) along with shrub vegetation. Otherwise, efforts may fail or lack cost-efficiency;
- (5) The Forest Service (GDF) should continue forest protection and fire suppression activities with a focus on dry seasons. Fire prevention and intervention plans need to be incorporated into the Kizildag's forest management plan. Otherwise, wildfires may cause massive CO₂ emissions in a very short time;
- (6) ALOS-2 PALSAR-2 image is a global mosaic data set that can be used in a practical way for carbon management of coniferous forests. VH polarization of Sentinel-1 is as important as HH polarization of ALOS-2 and it can be used as an alternative source for estimation of total carbon stock. As Sentinel-1 provides frequent data (every 6 or 12 days), it might be more useful to estimate the seasonal dynamics of total carbon stock in deciduous forests;
- (7) Researchers should further classify their broad LULC classes. The forest LULC class, for example, may be sub-classified as 'conifer & deciduous', 'productive & degraded', or 'even-aged & uneven-aged classes'. Thus, modellers can reach higher accuracy in their carbon estimates using SAR data;
- (8) The soil pool should be considered in SAR-based carbon modelling studies in sparsely covered forests. Since SAR can obtain information on soil-bound carbon, the inclusion of soil organic carbon stock may increase model accuracies. The majority of the carbon storage is composed of soil organic carbon in Mediterranean forest ecosystems;
- (9) Even without direct measurements and allometric equations, local forest inventory data can provide good estimates for total carbon storage in Mediterranean forests when used with L- and C-band SAR data. The approach used in this study should be repeated and transferred for different ecological regions and forest types to test its usability over a wide range. If these recommendations are followed, the potential of forests to absorb atmospheric CO₂ and store carbon will be further realized in Kizildag. Moreover, timber quality can be improved by timely silvicultural interventions which will, in turn, increase the use of industrial roundwood instead of low-quality fuelwood. Thus, carbon will remain stored in harvested wood products for a longer period of time. Considered on a large scale, the world's fossil fuel consumption will gradually be replaced by forest biomass as a renewable and carbon-neutral energy resource. In this manner, radar remote sensing still provides myriad opportunities to natural resource managers to mitigate the harmful effects of global warming and climate change.

Acknowledgements The authors thank the Republic of Turkey General Directorate of Forest (GDF) for providing the study area's forest management plan and its spatial database.

Open Access This article is licensed under a Creative Commons Attribution 4.0 International License, which permits use, sharing, adaptation, distribution and reproduction in any medium or format, as long as you give appropriate credit to the original author(s) and the source, provide a link to the Creative Commons licence, and indicate if changes

were made. The images or other third party material in this article are included in the article's Creative Commons licence, unless indicated otherwise in a credit line to the material. If material is not included in the article's Creative Commons licence and your intended use is not permitted by statutory regulation or exceeds the permitted use, you will need to obtain permission directly from the copyright holder. To view a copy of this licence, visit <http://creativecommons.org/licenses/by/4.0/>.

References

- Abdikan S (2018) Exploring image fusion of ALOS/PALSAR data and LANDSAT data to differentiate forest area. *Geocarto Int* 33(1):21–37
- Allen CD, Macalady AK, Chenchouni H, Bachelet D, McDowell N, Vennetier M, Kitzberger T, Rigling A, Breshears DD, Hogg EH, Gonzalez P, Fensham R, Zhang Z, Castro J, Demidova N, Lim J, Allard G, Running SW, Semerci A, Cobb N (2010) A global overview of drought and heat-induced tree mortality reveals emerging climate change risks for forests. *For Ecol Manage* 259(4):660–684
- Anderson K, Ryan B, Sonntag W, Kavvada A, Friedl L (2017) Earth observation in service of the 2030 agenda for sustainable development. *Geo Spat Inf Sci* 20(2):77–96
- Baskent EZ (2019) Exploring the effects of climate change mitigation scenarios on timber, water, biodiversity and carbon values: a case study in Pozantı planning unit, Turkey. *J Environ Manage* 238:420–433
- Behera MD, Tripathi P, Mishra B, Kumar S, Chitale VS, Behera SK (2016) Above-ground biomass and carbon estimates of *Shorea robusta* and *Tectona grandis* forests using QuadPOL ALOS PALSAR data. *Adv Space Res* 57(2):552–561
- Chave J, Chust G, Condit R, Aguilar S, Lao S, Perez R (2004) Error propagation and scaling for tropical forest biomass estimates. *Philos Trans R Soc Lond B* 359:409–420
- Cohen WB, Spies TA (1992) Estimating structural attributes of Douglas-fir—Western Hemlock forest stands from landsat and spot imagery. *Remote Sens Environ* 41:1–17
- Değermenci AS, Zengin H (2016) Investigating the spatial and temporal changes in forest carbon stocks: the case of Daday forest planning unit. *Artvin Coruh Univ J For Fac* 17(2):177–187
- Diñç M, Vatandaşlar C (2019) Analyzing carbon stocks in a Mediterranean forest enterprise: a case study from Kizildag, Turkey. *CERNE* 25(3):402–414
- Eriñç S (1984) *Climatology and its methods*. Gür-Ay Press, Istanbul, p 486 (in Turkish)
- Erkan N, Comez A, Aydın AC (2020) Litterfall production, carbon and nutrient return to the forest floor in *Pinus brutia* forests in Turkey. *Scand J For Res* 35(7):341–350
- ESA (2020) European Space Agency website. Available at: <https://sentinel.esa.int/web/sentinel/missions/sentinel-1>. Accessed 22 September 2020.
- FAO (2010) *Global Forest Resources Assessment 2010: Country report – Turkey*. Food and Agriculture Organization of the United Nations, Rome. Available at: <http://www.fao.org/3/al649E/al649E.pdf>. Accessed 23 September 2020.
- FAO (2015) *Global Forest Resources Assessment 2015: Main report*. Food and Agriculture Organization of the United Nations. Available at: <http://www.fao.org/3/a-i4808e.pdf>. Accessed 19 September 2020.
- FAO (2020) *Global Forest Resources Assessment 2020: Main report*, Rome. Available at: <https://doi.org/10.4060/ca9825en>
- Gao T, Zhu JJ, Yan QL, Deng SQ, Zheng X, Zhang JX, Shang GD (2018) Mapping growing stock volume and biomass carbon storage of larch plantations in Northeast China with L-band ALOS PALSAR backscatter mosaics. *Int J Remote Sens* 39(22):7978–7997
- GDF (2016) *Ecosystem-based functional forest management plan of the Kizildag Forest Enterprise (2016–2035)*. Republic of Turkey General Directorate of Forestry Press, Ankara, p 605 (in Turkish)
- GDF (2017) *The national guideline for the preparation of Ecosystem-based Multifunctional Forest Management Plans (Code No: 299)*. Republic of Turkey General Directorate of Forestry Press, Ankara, p 215 (in Turkish)
- Güner ŞT, Erkan N, Karataş R (2021) Effects of afforestation with different species on carbon pools and soil and forest floor properties. *Catena* 196:104871
- Günlü A, Ercanlı E (2018) Artificial neural network models by ALOS PALSAR data for aboveground stand carbon predictions of pure beech stands: a case study from northern of Turkey. *Geocarto Int* 35(1):17–28
- Hamdan O, Aziz HK, Hasmadi IM (2014) L-band ALOS PALSAR for biomass estimation of Matang Mangroves, Malaysia. *Remote Sens Environ* 155:69–78
- Hernando A, Puerto L, Mola-Yudego B, Manzanera JA, Garcia-Abril A, Maltamo M, Valbuena R (2019) Estimation of forest biomass components using airborne LiDAR and multispectral sensors. *iForest* 12:207–213
- Hu HF, Wang GG (2008) Changes in forest biomass carbon storage in the South Carolina Piedmont between 1936 and 2005. *For Ecol Manage* 255:1400–1408
- IPCC (2006) *Intergovernmental Panel on Climate Change Guidelines for National Greenhouse Gas Inventories*. In: Eggleston HS, Buendia L, Miwa K, Ngara T, Tanabe K (eds) Prepared by the National Greenhouse Gas Inventories Programme. IGES Press, Japan, p 367
- IPCC (2007) *Working group I contribution to the fourth assessment report of the Intergovernmental Panel on Climate Change*. In: Solomon S, Qin D, Marquis M, Averyt KB, Tignor M (eds) *Climate Change 2007: The physical basis*. Cambridge University Press, New York, p 996
- Jandl R, Lindner M, Vesterdal L, Bauwens B, Baritz R, Hagedorn F, Johnson DW, Minkinen K, Byrne KA (2007) How strongly can forest management influence soil carbon sequestration? *Geoderma* 137:253–268
- Lamloom SH, Savidge RA (2003) A reassessment of carbon content in wood: variation within and between 41 North American species. *Biomass Bioenergy* 25:381–388
- Le Toan T, Quegan S, Davidson MWJ, Balzter H, Paillou P, Papathanassiou K, Plummer S, Rocca F, Saatchi S, Shugart H, Ulander L (2011) The BIOMASS mission: Mapping global forest biomass to better understand the terrestrial carbon cycle. *Remote Sens Environ* 115:2850–2860
- Lillesand T, Kiefer R, Chipman J, Chipman J (2015) *Remote Sensing and Image Interpretation*, 7th edn. Wiley, New Jersey, p 736
- Liu Y, Gong W, Xing Y, Hu X, Gong J (2019) Estimation of the forest stand mean height and aboveground biomass in Northeast China using SAR Sentinel-1B, multispectral Sentinel-2A, and DEM imagery. *ISPRS J Photogramm Remote Sens* 151:277–289
- Meyer F (2019) *Spaceborne Synthetic Aperture Radar: Principles, Data Access, and Basic Processing Techniques*. In: Flores-Anderson AI, Herndon KE, Thapa RB, Cherrington (Eds) *The SAR Handbook: Comprehensive Methodologies for Forest Monitoring and Biomass Estimation*. Huntsville: SERVIR Global Press, p. 307.
- Mokany K, Raison JR, Prokushkin AS (2006) Critical analysis of root: shoot ratios in terrestrial biomes. *Glob Change Biol* 12:84–96
- Morel AC, Saatchi SS, Malhi Y, Berry NJ, Banin L, Burslem D, Nilus R, Ong RC (2011) Estimating aboveground biomass in forest and oil palm plantation in Sabah, Malaysian Borneo using ALOS PALSAR data. *For Ecol Manage* 262(9):1786–1798

- Mumcu Kucuker D (2020) Spatiotemporal changes of carbon storage in forest carbon pools of Western Turkey: 1972–2016. *Environ Monit Assess* 192:555
- Navarro JA, Algeet N, Fernández-Landa A, Esteban J, Rodríguez-Noriega P, Guillén-Climent ML (2019) Integration of UAV, Sentinel-1, and Sentinel-2 data for mangrove plantation aboveground biomass monitoring in Senegal. *Remote Sens* 11(1):77
- Njana MA (2017) Indirect methods of tree biomass estimation and their uncertainties. *South For* 79(1):41–49
- Nuthammachot N, Askar A, Stratoulas D, Wicaksono P (2020) Combined use of Sentinel-1 and Sentinel-2 data for improving aboveground biomass estimation. *Geocarto Int.* <https://doi.org/10.1080/10106049.2020.1726507>
- Omar H, Misman MA, Kassim AR (2017) Synergetic of PALSAR-2 and Sentinel-1A SAR polarimetry for retrieving aboveground biomass in Dipterocarp Forest of Malaysia. *Appl Sci* 7:675
- Ozkan K, Mert A, Gülsoy S (2007) Relationships between soil colour, soil structure and some soil properties in Beyşehir watershed. *Süleyman Demirel Univ J Fac For* 2(A):9–22
- Patel N, Majumdar A (2011) Comparative assessment of the relationship of satellite data with the above ground biomass of Sal trees (*Shorea robusta*) determined from phenologically different time periods. *Geo Spat Inf Sci* 14(3):177–183
- Pham TD, Yoshino K, Le NN, Bui DT (2018) Estimating aboveground biomass of a mangrove plantation on the Northern coast of Vietnam using machine learning techniques with an integration of ALOS-2 PALSAR-2 and Sentinel-2A data. *Int J Remote Sens* 39(22):7761–7788
- Saatchi SS, Harris LL, Brown S, Lefsky M, Mitchard ETA, Salas W, Zutta BR, Buermann W, Lewis SL, Hagen S, Petrova S, White L, Silman M, Morel A (2011) Benchmark map of forest carbon stocks in tropical regions across three continents. *Proc Natl Acad Sci USA* 108:9899–9904. <https://doi.org/10.1073/pnas.1019576108>
- Sanquetta CR, Corte APD, da Silva F (2011) Biomass expansion factor and root-to-shoot ratio for Pinus in Brazil. *Carbon Balance Manag* 6:6
- Saraçoğlu N (2010) Global climate change, bioenergy and energy forestry. Efil Press, Ankara, p 298 (in Turkish)
- Shimada M, Itoh T, Motooka T, Watanabe M, Shiraishi T, Thapa R, Lucas R (2014) New global forest/non-forest maps from ALOS PALSAR data (2007–2010). *Remote Sens Environ* 155:13–31
- Sinha S, Santra A, Das AK, Sharma LK, Mohan S, Nathawat MS, Mitra SS, Jeganathan C (2019) Accounting tropical forest carbon stock with synergistic use of space-borne ALOS PALSAR and COSMO-SkyMed SAR sensors. *Trop Ecol* 60:83–93
- Sinha S, Santra A, Sharma L, Jeganathan C, Nathawat MS, Das AK et al (2018) Multi-polarized Radarsat-2 satellite sensor in assessing forest vigor from above ground biomass. *J For Res* 29(4):1139–1145
- Sivrikaya F, Baskent EZ, Bozali N (2013) Spatial dynamics of carbon storage: a case study from Turkey. *Environ Monit Assess* 185:9403–9412
- SNAP (2019) Science Toolbox Exploitation Platform. Available at: <https://step.esa.int/main/toolboxes/snap/>
- Somogyi Z, Cienciala E, Mäkipää R, Muukkonen P, Lehtonen A, Weiss P (2007) Indirect methods of large-scale forest biomass estimation. *Eur J For Res* 126:197–207
- Sun W, Liu X (2020) Review on carbon storage estimation of forest ecosystem and applications in China. *For Ecosyst* 7:4
- Thapa RB, Watabene M, Motohka T, Shimada M (2015) Potential of high-resolution ALOS–PALSAR mosaic texture for aboveground forest carbon tracking in tropical region. *Remote Sens Environ* 160:122–133
- Tolunay D (2009) Carbon concentrations of tree components, forest floor and understorey in young *Pinus sylvestris* stands in north-western Turkey. *Scand J for Res* 24(5):394–402
- Tolunay D (2011) Total carbon stocks and carbon accumulation in living tree biomass in forest ecosystems of Turkey. *Turk J Agric for* 35:265–279
- Tolunay D, Çömez A (2008) Amounts of organic carbon stored in forest floor and soil in Turkey. In: Proceedings book of the national symposium on air pollution and control. Hatay/Turkey, 22–25 October 2008, pp. 750–765 (in Turkish).
- UN (2015) Transforming our world: The 2030 agenda for sustainable development (A/RES/70/1). Available at: https://www.un.org/en/development/desa/population/migration/generalassembly/docs/globalcompact/A_RES_70_1_E.pdf. Accessed 12 May 2021.
- UNFCCC (2016) Key decisions relevant for reducing emissions from deforestation and forest degradation in developing countries (REDD+). United Nations Framework Conventions on Climate Change. Available at: https://unfccc.int/files/land_use_and_climate_change/redd/application/pdf/compilation_redd_decision_booklet_v1.2.pdf. Accessed 24 September 2020.
- Vidal C, Alberdi I, Hernandez L, Redmond J (2016) National Forest Inventories: Assessment of Wood Availability and Use. Springer, Cham, p 847
- Wan P, Wang TJ, Zhang WM, Liang XL, Skidmore AK, Yan GJ (2019) Quantification of occlusions influencing the tree stem curve retrieving from single-scan terrestrial laser scanning data. *For Ecosyst* 6:43

Publisher's Note Springer Nature remains neutral with regard to jurisdictional claims in published maps and institutional affiliations.